Chinese Chemical Letters 37 (2026) 112487

Contents lists available at ScienceDirect

Chinese Chemical Letters

journal homepage: www.elsevier.com/locate/cclet

Facile construction of fluorescent probes for monitoring pH fluctuations in diabetic cataract

Chen Li[a,b,1], Zhe Liu[a,1], Jiuxiao Li[a], Yueping Ren[b,*], Kun Li[e], Weijie Chi[c], Ji-Ting Hou[a,*], Jianliang Shen[a,d,*]

[a] National Engineering Research Center of Ophthalmology and Optometry, Eye Hospital, Wenzhou Medical University, Wenzhou 325027, China
[b] National Clinical Research Center for Ocular Diseases, Eye Hospital, Wenzhou Medical University, Wenzhou 325027, China
[c] Collaborative Innovation Center of OneHealth, School of Chemistry and Chemical Engineering, Hainan University, Haikou 570228, China
[d] Zhejiang Key Laboratory of Ophthalmic Drug Discovery and Medical Device Research, Eye Hospital, Wenzhou Medical University, Wenzhou 325027, China
[e] Key Laboratory of Green Chemistry and Technology of Ministry of Education, College of Chemistry, Sichuan University, Chengdu 610064, China

ARTICLE INFO

Article history:
Received 31 December 2025
Revised 28 January 2026
Accepted 1 February 2026
Available online 1 February 2026

Keywords:
Fluorescent probe
Intracellular pH
Flavylium dye
Diabetic cataract
High glucose stress

ABSTRACT

Cataracts, particularly diabetic cataracts (DC), represent a significant cause of blindness, exacerbated by diabetes mellitus. Monitoring intracellular pH (pH_i) in human lens epithelial cells (HLECs) provides valuable insights into the pathogenesis of DC. This study introduces a novel phenol-armed flavylium-based fluorescent probe (FpH-2) for real-time pH monitoring in HLECs. The probe is facilely prepared to offer a reversible and highly sensitive fluorescence response to pH changes, with a pK_a value of 6.66. The probe's efficacy was demonstrated through its ability to monitor pH elevation under high glucose conditions, simulating diabetic stress. The study further investigates the effects of various clinical drugs on pH regulation in HLECs, offering new perspectives for managing DC. The findings suggest that pH_i serves as a critical parameter for investigating DC pathophysiology and pharmacology, offering potential for advancing early diagnostic and therapeutic strategies.

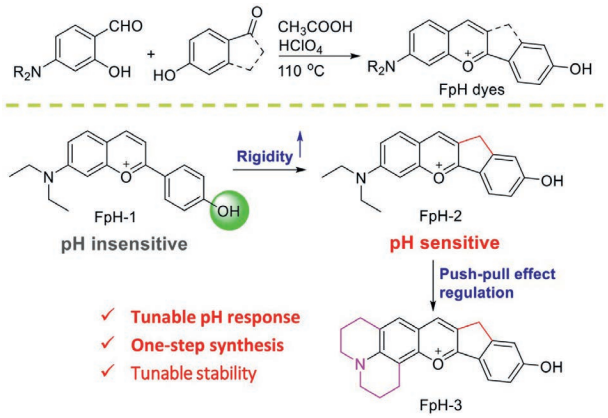
© 2026 Published by Elsevier B.V. on behalf of Chinese Chemical Society and Institute of Materia Medica, Chinese Academy of Medical Sciences.

Cataract is the leading cause of blindness with 15.2 million cases as per the 2020 Global Burden of Disease Study [1], and diabetes mellitus (DM) is a major risk factor for cataract development [2]. According to the International Diabetes Federation, the global diabetic population exceeds 285 million and is projected to rise to 439 million by 2030 [2]. The prevalence of diabetic cataract (DC) among diabetic patients is as high as 63% [3]. Compared to the general population, diabetic patients experience more rapid cataract progression [4] and a 2- to 5-fold higher incidence rate [5]. While uncomplicated cataracts can be effectively treated with mature surgical techniques, the clinical management of DC is more complex. Diabetic patients not only face a higher risk and faster progression of cataracts but also a significantly increased rate of postoperative complications, such as capsular contracture, posterior capsule opacification, and macular edema [6], imposing greater burdens on patients and healthcare systems. Therefore, in addition to surgical intervention, there is an urgent need to enhance preoperative drug management and early intervention for DC. Achieving this goal depends on a deeper understanding of its pathological mechanisms. In this context, the real-time and dynamic monitoring of key physiological parameters has become a research focus. Fluorescence detection techniques, particularly imaging methods based on activatable fluorescent probes, are ideally suited for this purpose by providing an indispensable tool for probing the subtle early pathological changes in human lens epithelial cells (HLECs) under diabetic stress [7–9].

Diabetes and its complications are linked to chronic inflammation and cellular dysfunction caused by persistent hyperglycemia. During DC progression, chronic hyperglycemia activates specific inflammatory pathways that contribute to HLECs injury and opacification [10]. Separately, as a critical microenvironment, intracellular pH (pH_i) is known to modulate inflammatory responses [11]. Integrating the above research advancement, we postulate that high glucose (HG) drives inflammation with pH_i disruption in HLECs. Coincidentally, HG has been reported to directly elevate cytosolic pH in pancreatic β-cells [12]. Therefore, constructing a powerful pH activatable fluorescent probe to monitor pH dynamics in HLECs under diabetic stress is immensely conducive to gain deep insight of the pathology of DC progression.

* Corresponding authors.
E-mail addresses: yuepingren@aliyun.com (Y. Ren), houjt2206@wmu.edu.cn (J.-T. Hou), shenjl@wiucas.ac.cn, sjl1@wmu.edu.cn (J. Shen).
[1] These authors contributed equally to this work.

https://doi.org/10.1016/j.cclet.2026.112487
1001-8417/© 2026 Published by Elsevier B.V. on behalf of Chinese Chemical Society and Institute of Materia Medica, Chinese Academy of Medical Sciences.



Scheme 1. Synthesis route of pH responsive fluorescent probes and their design strategy.

An ideal fluorescent probe for pH sensing should meet several requirements: (1) Reversible pH response for dynamic monitoring, (2) a stable fluorophore for reliable signal output, (3) a sufficient Stokes shift for crosstalk-free imaging by circumventing the overlap between excitation and emission spectra, (4) simple preparation with cheap and readily available chemicals for further translation, and (5) tunable structures for optimizing pH response. Although a mountain of pH-activated fluorescent probes has been documented so far, few of them integrate the above merits [13–27]. Therefore, constructing desirable pH-responsive structures is still in urgent demand.

Herein, we presented a one-step construction of fluorescent FpH dyes baring a phenol group as the pH regulating site. Properties of these probes, including stability, photophysical properties, and pH response could be tuned by exploiting commercial reactant analogues. FpH-2 with optimized performance was employed for monitoring pH fluctuations in HLECs, and confirmed the elevated pH_i induced by HG stimulation. Intriguingly, while we treated HG-stressed HLECs with various clinical drugs for cataract, different pH regulation outcomes were recorded, and the mechanisms of action of two anti-inflammatory agents were inspected, suggesting the potential of pH_i as a valuable index for investigating DC pathology and pharmacology.

Due to its sensitivity toward physiological pH and adjustable pK_a, phenol-armed fluorophores have been widely used in the design of pH-activatable probes [28]. However, these probes were synthesized through multiple steps, and usually needed strong Lewis acid-assisted demethylation of methoxy group to generate phenol tail. Here, starting from amino salicylaldehyde and 4-hydroxyacetophenone, we can facilely obtain phenol-installed flavylium dyes. The synthesis of these fluorophores was quite straightforward and the post-reaction processing was very simple by filtration and washing in high yields of 70%–80% (Scheme 1). The ^{1}H NMR, ^{13}C NMR, and HRMS spectra of these dyes were shown in Supporting information.

To our surprise, although FpH-1 showed an obvious bathochromic-shift in its absorption spectrum when the pH value of the test solution shifted from 5.0 to 8.0, indicating the formation of its deprotonation pattern, negligible increase in emission intensity (1.4 folds) and quantum yield was observed (Fig. S1 and Table S1 in Supporting information). We hypothesize that the free rotation of C–C bond between oxonium unit and phenol unit results in the nonradiative decay of the excited molecules, leading to a weak emission of its deprotonated form. Accordingly, a five-membered ring was introduced to strengthen the rigidity. As expected, an 8.8-fold intensity amplification was recorded for FpH-2 in the same conditions, demonstrating the rigidity-enhanced pH

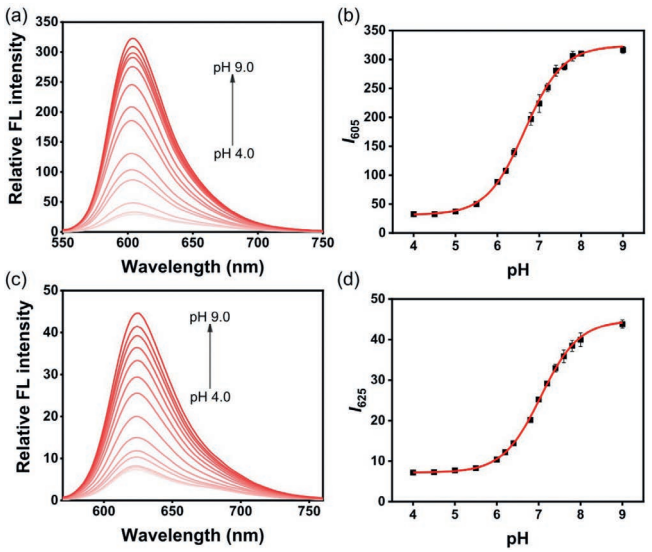


Fig. 1. (a) Emission spectra of FpH-2 (10 μmol/L) in buffer solutions with different pH values. Slit width: 2/2 nm; λ_{ex}: 530 nm. (b) Fluorescence titration curve of FpH-2 (I_{605}) in buffer solutions with different pH values. (c) Emission spectra of FpH-3 (10 μmol/L) in buffer solutions with different pH values. Slit width: 2/2 nm; λ_{ex}: 550 nm. (d) Fluorescence titration curve of FpH-3 (I_{625}) in buffer solutions with different pH values. The fluorescence tests were performed after a 30 min-incubation of the probes in different pH buffers.

sensitivity. Moreover, push-pull effect was tuned by enhancing the electron-donating ability of the amino substitute to give dye FpH-3, while a negative effect was observed that the intensity enhancement decreased to 4.4 folds. It might be ascribed to the weakened charge transfer from phenoxide anion to the electron-deficient oxonium center owing to the more electron-donating amino unit, thus suppressing the sensitivity of FpH-3 toward alkali pH. Additionally, the chemostability of these three dyes were checked. Upon the addition of common reactive oxygen and sulfur species under pH 4 and 8 conditions, the fluorescence of FpH-1 and FpH-2 were partially quenched by peroxynitrite ($ONOO^-$) under basic condition, while the fluorescence of FpH-3 was completely quenched under both circumstances, suggesting structure-tuned chemostability (Fig. S2 in Supporting information). Notably, such regulation of pH response and structure stability can be readily achieved by choosing commercial reactant analogues without further modification.

Subsequently, the optical behaviors of FpH-2 and FpH-3 toward pH alterations were examined in detail. Both probes emitted weak fluorescence at pH 3.0. Along with the stepwise increment in the pH values of B-R buffers, FpH-2 showed a gradual emission intensity enhancement at 605 nm and FpH-3 at 625 nm (Fig. 1). The pK_a values were calculated to be 6.69 ± 0.07 for FpH-2 and 7.02 ± 0.02 for FpH-3, respectively (Fig. S3 in Supporting information), suggesting these two probes are suitable for monitoring physiological pH. Under continuous irradiation at several excitation wavelengths for 30 min, both probes exhibited satisfying photostability with >90% intensity maintained (Fig. S4 in Supporting information). On the basis of the facts that FpH-2 showcases more obvious intensity changes and higher brightness at pH 8.0 than FpH-3 (Fig. S1 and Table S1), we used FpH-2 for the further experiments.

Subsequently, the emission spectra of FpH-2 in different solvents were recorded, including H_2O, dimethylsulfoxide (DMSO), acetonitrile (MeCN), *N,N*-dimethylformamide (DMF), methanol (MeOH), 1,4-dioxane, tetrahydrofuran (THF), dichloromethane (DCM), and glycerol. As shown in Fig. S5 (Supporting information), no regular relationship was observed between the fluorescence intensity of FpH-2 and solvent polarity or viscosity. A 2.4-fold inten-

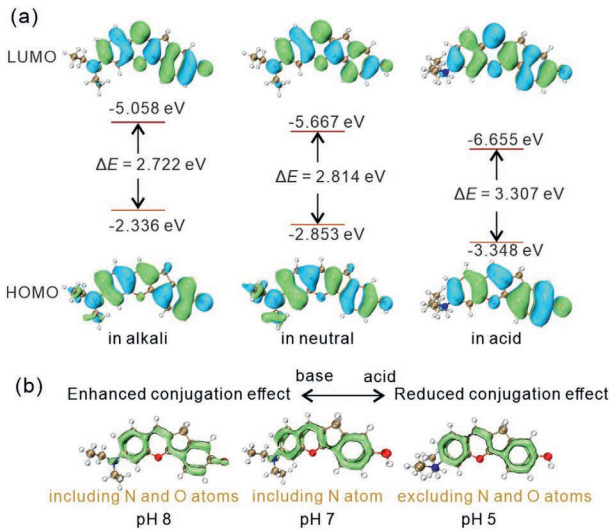


Fig. 2. (a) The calculated distributions, HOMO level, and LUMO level of FpH-2. (b) Iso-surface map of LOL-π of FpH-2 with isovalue 0.4 at B3LYP/Def2SVP level.

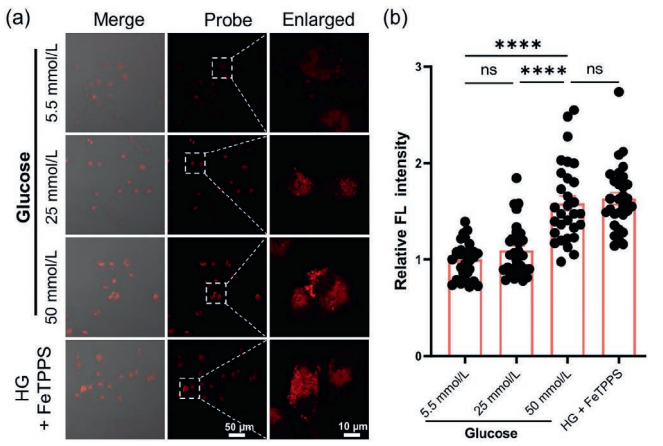


Fig. 3. Confocal fluorescence imaging of HLECs incubated with FpH-2. (a) Cells were treated with media containing different glucose concentrations for 24 h. Alternatively, cells were pretreated with FeTPPS (10 μmol/L) for 4 h prior to a 24-h exposure to 50 mmol/L-glucose medium. All cells were subsequently incubated with 5 μmol/L FpH-2 for 30 min prior to imaging. (b) Fluorescence intensity analysis for different groups. $\lambda_{ex} = 530$ nm and $\lambda_{em} = 540–680$ nm. Quantitative statistical analysis was performed using one-way ANOVA. Error bars: SEM. ns: no significance; $^{****}P < 0.0001$. Scale bar: 50 μm for original images and 10 μm for enlarged ones, respectively.

sity enhancement was measured in MeOH, which is much lower than that induced by alkaline pH. Therefore, the common environmental factors, such as intracellular viscosity or polarity, showed little influence on the probe's emission intensity.

To elucidate the underlying fluorescence response of FpH-2 toward pH, theoretical calculations were conducted. The geometries of FpH-2 were optimized using the B3LYP functional and the Def2SVP basis set, along with the SMD solvation mode [29,30]. Our results indicated that the highest occupied molecular orbital (HOMO) and the lowest unoccupied molecular orbital (LUMO) of FpH-2 were distributed across the entire molecule in neutral and alkaline conditions (Fig. 2a). In acidic conditions, however, the dimethylamine unit contributed minimally to the HOMO and LUMO. Furthermore, compared to neutral conditions, alkaline conditions led to an increase in both HOMO and LUMO energy levels, while protonation under acidic conditions significantly decreased these levels. Meanwhile, the energy gap of FpH-2 exhibited a slight decrease in alkaline conditions and a substantial increase in acidic conditions, which consists with the changes in absorption spectra.

The changes in fluorescence intensity of FpH-2 under acidic, neutral, and alkaline conditions can be explained by the distribution of π electrons, characterized using the Localized Orbital Locator (LOL-π) [31]. The LOL function identifies regions of high electron localization. Our results indicate that the LOL-π for FpH-2 exhibits a narrower distribution in acidic conditions compared to neutral conditions (Fig. 2b). Specifically, the nitrogen and the oxygen atoms do not participate in electron conjugation in acidic conditions. In contrast, under alkaline conditions, both the nitrogen and the oxygen atoms significantly contribute to electron conjugation. This enhanced conjugation effect results in amplified fluorescence intensity of FpH-2 in alkaline conditions compared to both neutral and acidic conditions.

To precisely assess pH_i changes within HLECs under diabetic stress, obtaining a pH_i calibration curve is imperative. Prior to this, the cytotoxicity of FpH-2 was evaluated in HLECs. As shown in Fig. S6 (Supporting information), even when the probe concentration reached up to 25 μmol/L, the cell viability still exceeded 80 %. In addition, after continuous imaging for thirty scans, there was almost no loss in the fluorescence intensity, affirming the desirable photostability of the probe (Fig. S7 in Supporting information). Subsequently, cells underwent a 30-minute pretreatment with FpH-2. Following this, the pH calibration curve was generated by substituting the medium with buffer solutions spanning pH values from 4.5 to 8.0 in conjunction with a known H^+/K^+ ion carrier (Nigerian mycoplasma), and imaging the cells after a 30-min incubation period. As depicted in Fig. S8 (Supporting information), the fluorescence intensity in the cells exhibited a linear increase with the elevation of pH_i from 4.5 to 8.0, signifying the consistent pH dependency of FpH-2′s fluorescence within living cells. The co-localization assay was also performed. As shown in Fig. S9 (Supporting information), the fluorescence of FpH-2 showed poor overlap with that of Lyso Tracker Green for lysosomes or Mito Tracker Green for mitochondria, suggesting that the probe was distributed across the whole cytoplasm. Therefore, its pH_i response range of 4.5–8.0 is quite suitable for the further mapping.

Cellular DC model was established in HLECs by incubation with high concentrations of glucose [32]. As shown in Fig. 3, along with the elevated glucose concentrations from 5.5 mmol/L to 50 mmol/L, the fluorescence intensity within the cells obviously increased, revealing rising pH_i values in HLECs during diabetic stress. As $ONOO^-$ is endogenously generated during DC progression [33], FeTPPS, a $ONOO^-$ scavenger [34], was pretreated with HLECs following by 50 mmol/L glucose (HG) stimulation. It was confirmed that the removal of $ONOO^-$ by FeTPPS showed neglectable effects on the fluorescence intensity of FpH-2 in HG-treated HLECs, suggesting that endogenous $ONOO^-$ negligibly affects the imaging accuracy of FpH-2. This is might be ascribed to the much lower concentrations of endogenous $ONOO^-$ than that in the solution test (100 μmol/L). Considering that the pH_i level usually undergoes immediate changes along with the onset of pathology, we thus propose that pH_i can be a valuable index for investigating the pathology of DC.

Given the elevated pH in the HLECs, we sought to evaluate the pH_i regulation efficacy of various drugs in treating DC. This study examined two antidiabetic agents: Glibenclamide, which enhances pancreatic β-cell insulin secretion [35], and metformin, which improves tissue insulin sensitivity [36]. To address heightened ocular oxidative stress caused by elevated aqueous glucose levels during DC progression [37], we also investigated two anti-inflammatory agents, MCC950 and SRT1720, and an antioxidant butyrophenone [38]. Also, interventions were conducted using the aldose reductase inhibitor epalrestat and the advanced glycation end product inhibitor naringin. Epalrestat inhibits lens opacification by correct-

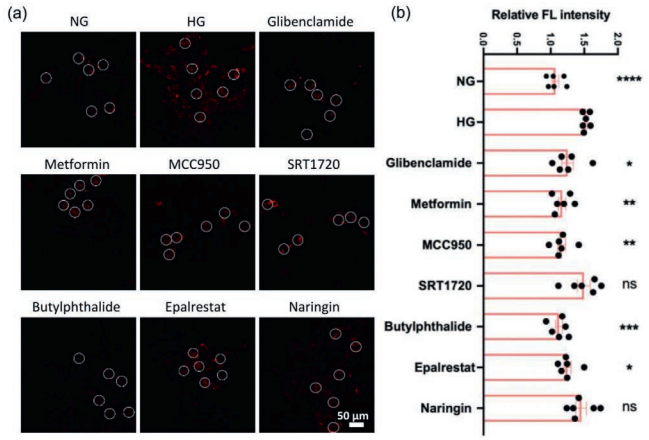


Fig. 4. Fluorescent images of HLECs stained with FpH-2 following different treatments. (a) HLECs were stimulated with normal or high glucose concentrations for 24 h. Subsequently, cells were treated for 2 h with glibenclamide (100 μmol/L), metformin (100 μmol/L), MCC950 (1 μmol/L), SRT1720 (0.5 μmol/L), butylphthalide (10 μmol/L), epalrestat (10 μmol/L), or naringin (10 μmol/L), followed by a 24-h treatment with 50 mmol/L glucose prior to staining with the probe for fluorescence imaging. (b) Fluorescence intensity analysis for different treatment conditions. $\lambda_{ex} = 530$ nm and $\lambda_{em} = 540–680$ nm. Quantitative statistical analysis was performed using one-way ANOVA. Error bars: SEM. ns: no significance; $^{*}P < 0.05$, $^{**}P < 0.01$, $^{***}P < 0.001$. Scale bar: 50 μm.

ing aberrant glucose metabolism, and naringin delays cataract formation by mitigating lens protein denaturation [39,40].

Representative regions from both normal and drug-stimulated cells were selected to analyze their relative fluorescence intensity. In this experiment, HLECs were first treated with different drugs for 2 h and then exposed to 50 mmol/L glucose (HG condition) for 24 h to induce a hyperglycemic environment before imaging analysis. As illustrated in Fig. 4, the relative fluorescence intensity under the normal glucose (NG, 5.5 mmol/L) condition was significantly lower than that in the HG group. Compared to the HG group, the intensity was obviously reduced in the cells treated by glibenclamide, metformin, MCC950, butylphthalide, and epalrestat, whereas the SRT1720 and naringin treatment showed no significant effects on the intensity. These results imply that although all of these drugs exhibit certain treatment efficacy in treating DC, their abilities to regulate pH_i in HLECs differ.

Among these drugs, MCC950 and SRT1720 aroused our interest. Both of them are anti-inflammatory agents, but MCC950 can inhibit the pH_i increment under HG stimulation while SRT1720 fails (Fig. 4), suggesting their differentiated mode of action which leads to different regulation effects on pH_i. MCC950 functions as a direct inhibitor of NLRP3 inflammasome that is a key mediator in immune and inflammatory responses and plays a crucial role in the diabetic complications [41–43]. SRT1720 indirectly modulates the NLRP3 inflammasome by activating SIRT1 [44].

Activation of NLRP3 inflammasome-related regulatory pathways and apoptosis-associated speck-like protein containing a CARD recruitment induces pyroptosis and subsequent secretion of the biologically active IL-1β p17 fragment [45], contributing to hyperglycemia-induced cataract formation [46]. In cellular inflammatory responses, cytosolic pH acts as regulatory signals and correlates with IL-1β [11]. Our experimental results confirm that the pH_i in HLECs was elevated under HG stimulation. Western-blot analysis showed a progressive increase in NLRP3 expression and elevated IL-1β p17 secretion with rising glucose concentrations in HLECs (Figs. 5a-c). Pretreatment with MCC950 and SRT1720 largely attenuated the expression of NLRP3, affirming their anti-inflammatory efficacy and the independence between NLRP3 overexpression and pH elevation in HLECs under diabetic stress. Intriguingly, MCC950 significantly suppressed IL-1β p17 expression in HLECs under HG conditions, whereas SRT1720 exhibited limited inhibitory efficacy in this context (Figs. 5d-f). In combination with the fact that MCC950 prohibits the pH_i elevation more apparently than SRT1720 (Fig. 4), we speculate that the formation of IL-1β p17 through the cleavage of IL-1β contributes to the pH elevation during DC progression, which has not been discussed before. Considering that SRT1720 can partially suppress the IL-1β p17 expression but barely reduce pH_i values in HLECs under diabetic stress, we hypothesize that there must be other factors regulating the intracellular acidity in DC.

In conclusion, this study highlights the development of a flavylium-based fluorescent probe FpH-2, which enables precise monitoring of pH_i dynamics in HLECs under diabetic conditions. The probe demonstrated excellent stability, photophysical properties, and sensitivity to pH changes, making it an ideal candidate for studying the pathophysiology of DC. Through this tool, we identified a significant elevation in pH_i in HLECs exposed to HG, a hallmark of diabetic stress. Moreover, the differential efficacy of various clinical drugs in regulating pH_i underscores the complexity

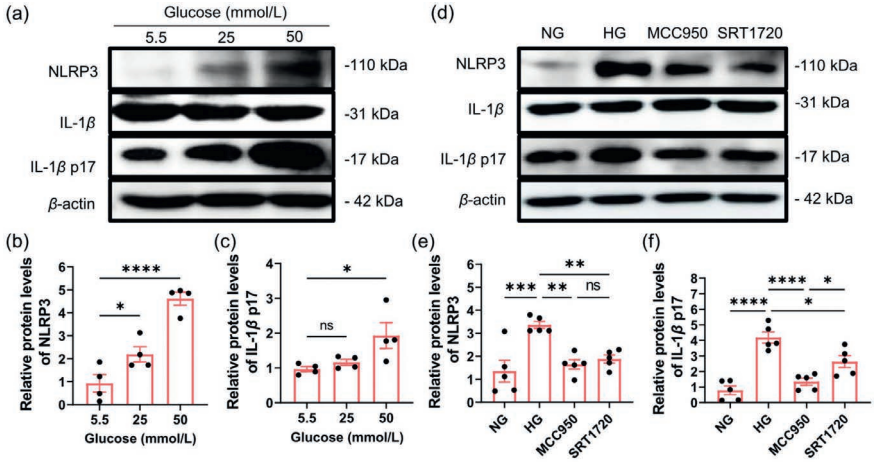


Fig. 5. Correlation between HLECs and pyroptosis under different stimulation conditions. (a) Western blot analysis of relevant proteins in HLECs following stimulation with varying glucose concentrations. Statistical results of (b) NLRP3 and (c) IL-1β p17 protein expression levels in HLECs following stimulation with varying glucose concentrations. (d) Western blot analysis of relevant proteins in HLECs following stimulation with varying glucose concentrations and drugs. Statistical results of (e) NLRP3 and (f) IL-1β p17 protein expression levels in HLECs following stimulation with different glucose concentrations and drugs. Data were analyzed by using one-way ANOVA. $n = 5$; ns: no significance; $^{*}P < 0.05$, $^{**}P < 0.01$, $^{***}P < 0.001$, $^{****}P < 0.0001$. Error bars: SEM.

of therapeutic interventions for DC treatment, offering valuable insights into their distinct modes of action. Especially, it is uncovered that NLRP3 overexpression in HLECs under diabetic stress barely affects pH_i while IL-1β p17 expression is probably associated with the pH_i fluctuations in this pathological process. The limitation of this work is that the underlying regulatory factors for the pH_i in HLECs under diabetic stress have not been excavated. Briefly, by integrating pH_i as a key index for cellular health, this research contributes to a deeper understanding of DC progression and lays the groundwork for developing more effective diagnostic and therapeutic approaches for managing this common complication of diabetes.

CRediT authorship contribution statement

Chen Li: Writing – original draft, Investigation, Data curation. **Zhe Liu:** Investigation, Data curation. **Jiuxiao Li:** Investigation. **Yueping Ren:** Supervision. **Kun Li:** Supervision. **Weijie Chi:** Writing – original draft, Software, Methodology, Data curation. **Ji-Ting Hou:** Writing – review & editing, Supervision, Investigation, Funding acquisition, Conceptualization. **Jianliang Shen:** Writing – review & editing, Supervision, Conceptualization.

Declaration of competing interest

The authors declare that they have no known competing financial interests or personal relationships that could have appeared to influence the work reported in this paper.

Acknowledgment

This work was financially supported by Wenzhou Medical University (No. KYYW202206).

Supplementary materials

Supplementary material associated with this article can be found, in the online version, at doi:10.1016/j.cclet.2026.112487.

References

[1] K. Pesudovs, V.C. Lansingh, J.H. Kempen, et al., Eye 38 (2024) 2229–2231.
[2] A. Pollreisz, U. Schmidt-Erfurth, J. Ophthalmol. 2010 (2010) 608751.
[3] M.B. Janghorbani, R.B. Jones, S.P. Allison, Ophthalmic Epidemiol. 7 (2000) 13–25.
[4] S. Kato, T. Oshika, J. Numaga, et al., Am. J. Ophthalmol. 130 (2000) 354–355.
[5] L. Li, X.H. Wan, G.H. Zhao, BMC Ophthalmol. 14 (2014) 94.
[6] N.M. Haddad, J.K. Sun, S. Abujaber, et al., Semin. Ophthalmol. 29 (2014) 329–337.
[7] K. Grover, A. Koblova, A.T. Pezacki, et al., Chem. Rev. 124 (2024) 5846–5929.
[8] H. Li, H. Kim, F. Xu, et al., Chem. Soc. Rev. 51 (2022) 1795–1835.
[9] M. Xian, Y. Wang, C. Du, et al., Acc. Chem. Res. 58 (2025) 2804–2814.
[10] Z. Guo, X. Ma, R.X. Zhang, et al., Adv. Ophthalmol. Pract. Res. 3 (2023) 180–186.
[11] Y.J. Chen, R.C. Shi, Y.C. Xiang, et al., Signal Transduct. Target. Ther. 9 (2024) 367.
[12] Y. Fang, H. Feng, B. Zhang, et al., Cell Metab. 36 (2024) 1237–1251 E4.
[13] J. Ma, R. Sun, K. Xia, et al., Chem. Rev. 124 (2024) 1738–1861.
[14] S. Wang, W.X. Ren, J.T. Hou, et al., Chem. Soc. Rev. 50 (2021) 8887–8902.
[15] Y. Liu, D. Zhang, Y. Qu, et al., Chem. Biomed. Imaging 2 (2024) 81–97.
[16] J. Wang, J.T. Yan, S.T. Zeng, et al., Anal. Chem. 95 (2023) 16609–16617.
[17] H. Zhang, F.-F. Xiang, D.-H. Zhou, et al., Sci. Bull. 70 (2025) 4219–4229.
[18] P.M. Sonawane, N. Jain, A. Roychaudhury, et al., Talanta 298 (2025) 128963.
[19] L.J. Gui, K.Z. Wang, Y.X. Wang, et al., Chin. Chem. Lett. 34 (2023) 107586.
[20] B. Feng, Y.S. Ma, F. Zheng, et al., Chem. Eng. J. 464 (2023) 142554.
[21] F. Deng, H.R. Zhang, K. Yang, et al., Microchem. J. 197 (2024) 109772.
[22] A. Mukherjee, P.C. Saha, R.S. Das, et al., ACS Sens. 6 (2021) 2141–2146.
[23] P. Wu, Y. Zhu, S. Liu, et al., ACS Cent. Sci. 7 (2021) 2039–2048.
[24] S. Chakraborty, M.M. Joseph, S. Varughese, et al., Chem. Sci. 11 (2020) 12695–12700.
[25] M.H. Lee, J.H. Han, J.H. Lee, et al., Angew. Chem. Int. Ed. 52 (2013) 6206–6209.
[26] Y. Urano, D. Asanuma, Y. Hama, et al., Nat. Med. 15 (2009) 104–109.
[27] T. Kowada, J. Kikuta, A. Kubo, et al., J. Am. Chem. Soc. 133 (2011) 17772–17776.
[28] J. Han, K. Burgess, Chem. Rev. 110 (2010) 2709–2728.
[29] A.V. Marenich, C.J. Cramer, D.G. Truhlar, J. Phys. Chem. B 113 (2009) 6378–6396.
[30] M.E. Frisch, G. Trucks, H. Schlegel, et al., Gaussian 16, Revision C. 01, Gaussian, Inc., Wallingford CT, 2016.
[31] T. Lu, F. Chen, J. Comput. Chem. 33 (2012) 580–592.
[32] S. Guo, C. Li, L. Lian, et al., ACS Sens. 8 (2023) 3882–3891.
[33] S.S. Moghadam, A. Oryan, B.I. Kurganov, et al., Int. J. Biol. Macromol. 103 (2017) 74–88.
[34] X. Hu, C. Yao, B. Wang, et al., Angew. Chem. Int. Ed. 64 (2025) e202503579.
[35] Y. Qiu, Y. Yang, Y. Wei, et al., iScience 23 (2020) 101446.
[36] M. Foretz, B. Guigas, L. Bertrand, et al., Cell Metab. 20 (2014) 953–966.
[37] Y. Chen, X.B. Sun, H.E. Lu, et al., Arch. Pharm. Res. 40 (2017) 88–95.
[38] Z. Ma, J. Liu, J. Li, et al., Int. Immunopharmacol. 85 (2020) 106582.
[39] V.R. Drel, P. Pacher, T.K. Ali, et al., Int. J. Mol. Med. 21 (2008) 667–676.
[40] P.F. Kador, D. Betts, M. Wyman, et al., Am. J. Vet. Res. 67 (2006) 1783–1787.
[41] C. Geraci, M. Guarneri, R. Arsena, et al., J. Nephrol. 21 (2008) 175–179.
[42] Z.W. Yu, J. Zhang, X. Li, et al., Life Sci. 240 (2020) 117138.
[43] H. Chen, X. Zhang, N. Liao, et al., Invest. Ophthalmol. Vis. Sci. 59 (2018) 978–985.
[44] L. Lian, Z. Le, Z. Wang, et al., Invest. Ophthalmol. Vis. Sci. 64 (2023) 16.
[45] H.H. Tseng, C.T. Vong, Y.W. Kwan, et al., Sci. Rep. 6 (2016) 35016.
[46] K. Schroder, R. Zhou, J. Tschopp, Science 327 (2010) 296–300.